Surface-Wave Suppression of Resonance-Type Periodic Structures

Ruey Bing Hwang, *Member, IEEE,* and Song Tsuen Peng, *Fellow, IEEE*

***Abstract*—Periodic structures of the resonance type are investigated with a focus on the utilization of structure dispersion to achieve a wide-band operation for the surface-wave suppression. Both approximate and exact formulations are presented to illustrate wave processes involved in the resonant structure and to develop useful criteria for design purpose. In addition, experiments are performed to verify the phenomena with stopband and leakage associated with the resonance-type periodic structures.**

***Index Terms*—Corrugated metal surface, periodic structures, resonance-type periodic structures, surface-wave suppression.**

I. Introduction

We present here an investigation of the guiding characteristics of resonance-type periodic structures that are composed of infinitely many identical cavities filled with dielectric medium. For example, a corrugated metal surface may be viewed as a structure consisting of infinitely many identical cavities, each having an aperture that is open to the air half-space. In fact, such a class of corrugated metal surface had been rigorously analyzed and was published in numerous papers since the mid-20th century [1]–[13]. For instance, the propagation of surface waves along a uniform planar corrugated structure, under TM mode operation, has been investigated in the 1950s by Rotman [1], Elliott [2], Hurd [3], and Vainshtein [4]. Although the surface wave behaviors associated with the corrugated metal surface are well known, we revisit, in this paper, the structure and would like to present some interesting phenomena that had not been observed previously.

The main purpose of this paper is to investigate the effect of such strong dispersion on the propagation characteristics of the type of periodic structures. Our interest here is to build up the fundamental understanding of waves guided by the resonance-type periodic structures and to explore new and interesting phenomena that are not realized in the case of weak dispersion.

For low frequency applications, the theoretical analyzes of such a structure had been mostly based on the model of uniform impedance surface, neglecting the effect of the periodicity. As far as a periodic structure is concerned, there are two important factors affecting their guiding characteristics: the basic dispersion and the period of the structure. Since a cavity may be in resonance at different frequencies, a periodic structure of the resonance type will exhibit strong dispersion.

The excitation of surface waves may degrade the performance of microwave or millimeter wave circuits and antennas; such as the mutual coupling between antenna elements resulting in the alteration of the radiation pattern and the reduction of radiation efficiency of antennas. Several methods had been developed for the surface-wave suppression in the literatures, such as: the concept of artificial soft and hard surfaces has been introduced to generally characterize the interaction between the load surface and surface waves. In particular, various soft surfaces were proposed by Kildal to suppress the lateral lobe in monopole antennas [11]–[13]. The partial removal of the substrate underneath the circuitry or antenna is used to reduce the excitation of surface wave [14]–[16] and the utilization of the Bragg reflection on periodic structures [17]–[21]. Recently, a planar periodic structure fabricated by the printed-circuit technology had been developed for the application as a high impedance surface that suppresses surface waves with a complete stopband [17]–[19]. The physical mechanism of the high-impedance surface may be explained on a basis of the distributed *LC*-resonance circuit in a unit cell, but the validity and generality of the model of periodic structures remains to be better understood.

The class of corrugated structures can be formulated rigorously by the method of mode matching as an electromagnetic boundary-value problem. The total fields above the corrugated surface can be expressed in the form of Fourier series, while those within the corrugated region can be expressed as a superposition of the complete set of parallel-plate waveguide modes. With an incident plane wave, the continuity of the tangential components of the total fields leads to a set of linear equations to determine the amplitudes of the Fourier components in the air region. The condition for the existence of a nontrivial solution in the absence of the incident wave yields the dispersion relation of the waveguiding structure; thus, this problem is considered completely solved.

Based on the exact approach described above, we have carried out extensive numerical results to identify and explain physical phenomena associated with the structures. The dispersion characteristics are displayed in the form of the Brillouin diagram, with both phase and attenuation constants included. In particular, the bound-wave regions are carefully examined, and very interesting numerical results are obtained to explain the effect of strong dispersion on the waveguiding characteristics and to explore its potential applications. In short, the main objectives of this research work are: 1) to clarify the basic concepts and

Manuscript received January 10, 2001; revised May 9, 2002. This work was supported by the Ministry of Education and National Science Council, Taiwan, R.O.C., under Grants 89-E-FA06-2-4 and 90WFA0600230.

R. B. Hwang is with the Graduate Institute of Communication Engineering, National Chi Nan University, Nantou, Taiwan, R.O.C. (e-mail: rbhwang@ncnu.edu.tw).

S. T. Peng is with the Microelectronics and Information Systems Research Center, National Chiao-Tung University, Hsinchu, Taiwan, R.O.C.

Digital Object Identifier 10.1109/TAP.2003.811470

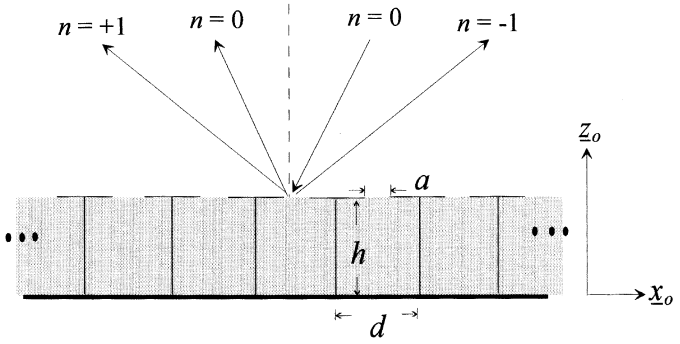

Fig. 1. Scattering of plane waves by corrugated metal surface.

to evaluate the validity of modeling a periodic structure as an impedance surface, 2) to provide a clear physical picture of the wave processes involved in the resonance-type periodic structures, and 3) to develop useful criteria for the design of the periodic structures by utilizing the structural resonance for the broadband operation of the Bragg reflection.

II. Statement of Problem

Fig. 1 shows the configuration of a periodic structure that is composed of infinitely many identical cavities, each with an opening to the air half-space. With the coordinate system attached, the corrugated structure has a period d in the x direction and is uniform in the y direction. Each cavity may be viewed as a parallel-plate waveguide that is completely short-circuited at one end and partially short-circuited at the other end. The opening of each cavity has the width a and is centrally located on the top cover. Furthermore, the structure has an infinite length and has a height h. Such a structure had been modeled as an impedance surface to explain Wood's anomaly in the scattering of light. Assuming that both the structure and the incident wave are invariant in the y direction, we may treat the guiding of either TE or TM wave separately as a boundary-value problem. For practical interest, we try to keep the height of the corrugated structure sufficiently small, so that we may consider the TM polarized wave only, although our theory applies to the other polarization as well.

III. Method of Analysis

Since the structure under consideration is periodic along the x direction, a set of Fourier components or space harmonics is generated in the air region, with the longitudinal propagation constant of the n^{th} harmonic given by:

$$k_{xn} = k_x + n\frac{2\pi}{d}, \quad \text{for } n = 0, \pm 1, \pm 2, \ldots \tag{1}$$

where k_x is the propagation constant of the fundamental harmonic. In the air region, the general field solutions can be expressed as a superposition of the complete set of space harmonics, each of which propagates independently as a plane wave. On the other hand, in the corrugated region, the general field solutions can be easily represented as a superposition of the parallel-plate waveguide modes. By imposing the boundary conditions at the structure-air interface, $z = 0$, the existence of nontrivial solution in the absence of any incident wave leads to the transverse-resonance condition:

$$\det \left\lfloor P^{+}\left(k_x^*\right) Z_{in} P(k_x) + Z_a \right\rfloor = 0 \tag{2}$$

Such an equation defines the dispersion relation to determine the guided modes of the corrugated structure. Here, P is the coupling matrix with its elements obtainable analytically from the overlap integrals of the waveguide modes in the corrugated region and the space harmonics in the air region. Z_{in} is a diagonal matrix with the input impedance of the m^{th} parallel-plate waveguide mode as its m^{th} diagonal element, as given by:

$$Z_m^{(in)} = j\frac{\omega\varepsilon_o}{\kappa_m} tan\kappa_m h, \quad for\, m = 0, 1, 2, \ldots \tag{3}$$

where κ_m is the propagation constant in z direction of the m^{th} parallel-plate waveguide mode, and can be given as:

$$\kappa_m = k_o\sqrt{\varepsilon_s - \left(\frac{m\lambda}{2d}\right)^2} \tag{4}$$

Finally, Z_a is also a diagonal matrix with the wave impedance of the n^{th} space harmonic in the air region as its n^{th} diagonal element, as given by:

$$Z_n = \frac{k_{zn}}{\omega\varepsilon_o} \tag{5}$$

where k_{zn} is the propagation constant in the z direction of the n^{th} space harmonic. Thus, all the parameters in (2) are defined.

The dispersion relation in (2) is a determinantal equation of infinite order; it requires a suitable truncation to a finite order to yield numerical results. We have implemented a computer code on the basis of the exact formulation described above to determine the dispersion roots of the structure. The results are obtained systematically for various structure as well as incident parameters, in order to identify the physical mechanism involved and their physical implications.

IV. Numerical Results and Discussions

Base on the exact formulation described in the preceding section, we are now in a good position to carry out both qualitative and quantitative analyzes of the guiding characteristics of the corrugated metal surface. Before embarking on an elaborate numerical analysis, it is instructive to consider first the approximation by only one single mode in the parallel-plate waveguides. In doing so, the periodic structure may then be replaced by a uniform surface impedance that is determined by the input impedance as given in (3) for any waveguide mode of interest. The propagation constant of a surface wave guided by such an impedance surface can be obtained explicitly as:

$$k_{sw}^{(m)} = \sqrt{k_o^2 + \kappa_m^2 \tan^2 \kappa_m d} \tag{6}$$

Graphically, such a simple expression can be plotted into curves in the form of the Brillouin diagram, and the results are shown in heavy solid lines in colors in Fig. 2 for the lowest four modes, $m = 0$, 1, 2, and 3. As far as the periodic structure is concerned, these four curves and their reflection-symmetric ones with respect to the vertical axis may be regarded as the basic dispersion

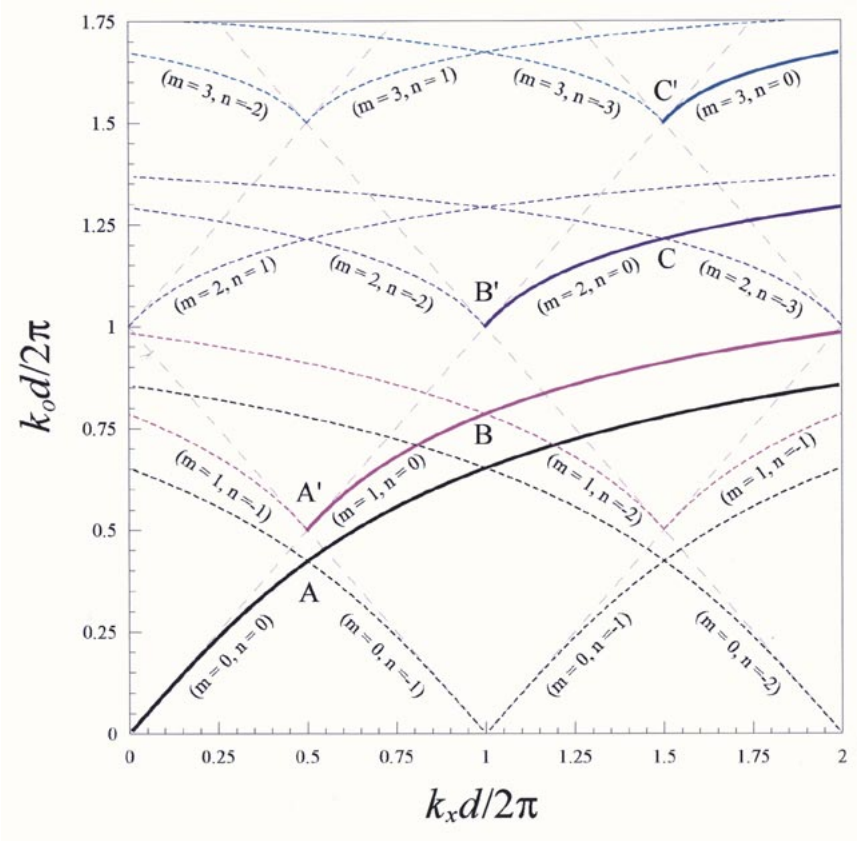

Fig. 2. Unperturbed dispersion curves for the case of $h = 0.21d$ and $a = d$.

curves. For the overall structure, the Brillouin diagram can be constructed approximately by periodic translations of the basic dispersion curves along the horizontal axis to form the set of unperturbed ones. It is well known that strong interactions of waves may take place in the vicinities of the intersection points among the unperturbed dispersion curves, as marked by the A's, B's, and C's in Fig. 2. This allows us to identify easily possible physical effects associated with the structure and will be particularly useful for an initial design in practice.

It is well known that the Bragg phenomenon will occur at $k_x d/2\pi = 0.5n$, where n is an integer running from negative to positive infinity. For example, in Fig. 2, the first-order interaction takes place between the fundamental harmonic $(n = 0)$ and the first higher harmonic $(n = -1)$ in the vicinity of the intersection point A. Similarly for the next two higher-order modes, the intersection points are marked by B for $m = 1$ and C for $m = 2$. It is interesting to note that at the point marked by A$'$, two physical processes take place: one is the onset of propagation of the first higher order mode $(m = 1)$ and the other is the intersection point of two harmonics, $n = 0$ and $n = -1$, of the same mode. Similar explanation may be given for the points marked by B$'$ and C$'$ for the higher-order modes. Thus, we should expect stopbands to arise in the vicinities of not only the points marked by A, B, and C, but also those marked by A$'$, B$'$ and C$'$.

Based on the exact dispersion relation in (2), we have carried out a systematic evaluation of the guiding characteristics of the corrugated structure, and the results are displayed in the form of the Brillouin diagram in Fig. 3 for both real and imaginary parts of k_x. It is noted that the shaded area is the bound-wave region; otherwise, it is the radiating or leaky-wave region. When the frequency is increased from a small value, the real part of k_x falls first in the bound-wave region and the imaginary part of k_x stays zero until the occurrence of the stopband. Thereafter, the guided wave enters into the leaky-wave region, and the value of k_x stays complex, with nonzero imaginary part in general.

Returning back to Fig. 2, if we start again from the low frequency range, the dispersion curve should follow closely that of the fundamental mode up to the vicinity of the intersection point A, where a stopband occurs; this is indeed the case, as is evident in Fig. 3. It is striking to observe that when the frequency is increased further above the first stopband, the actual dispersion curve does not follow that of the fundamental mode any longer; it jumps to that of the next high-order mode. Such a phenomenon of jumping from one mode to the next higher mode seems to be always the case, as is evidently seen in the vicinities of the points marked by B and C. This means physically that in a different frequency range, the model of the impedance surface has to take the input impedance of a different waveguide mode. Thus, we may conjecture that the fields inside the corrugated regions are dominated by a single mode that may change from one to another, depending on the operating frequency. Furthermore, comparing Figs. 2 and 3, we observe that the first stopband exists over the range of frequency between the pair of points A and A$'$. In other words, contrary to our original expectation, we do not have two stopbands separately around the points marked by A and A$'$. A physical interpretation may be given as follows. When the fundamental mode reaches the stopband region, the real part of k_x

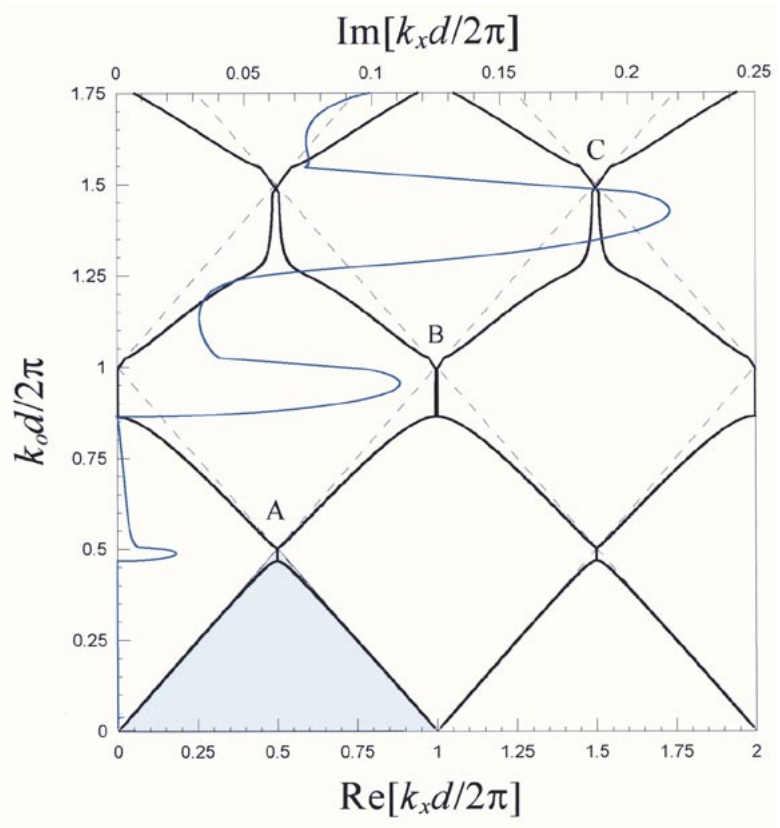

Fig. 3. Brillouin diagram of a corrugated metal surface for the case of $h = 0.21d$ and $a = d$.

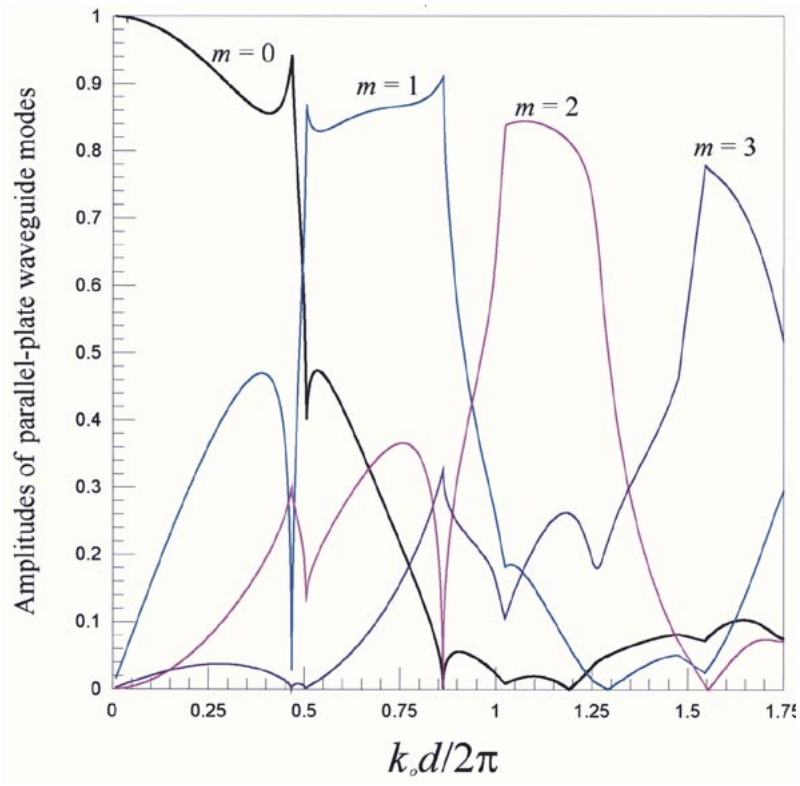

Fig. 4. Variation of amplitudes of parallel-plate waveguide modes against normalized frequency $k_o d/2\pi$ for the corrugated metal surface with the parameters: $h = 0.21d$ and $a = d$.

in the air region matches with the transverse propagation constant of the first higher mode of the parallel-plate waveguides, at the value $k_x d/2\pi = 0.5$. With such a phase matching condition, the fundamental and the first-order modes are strongly coupled,

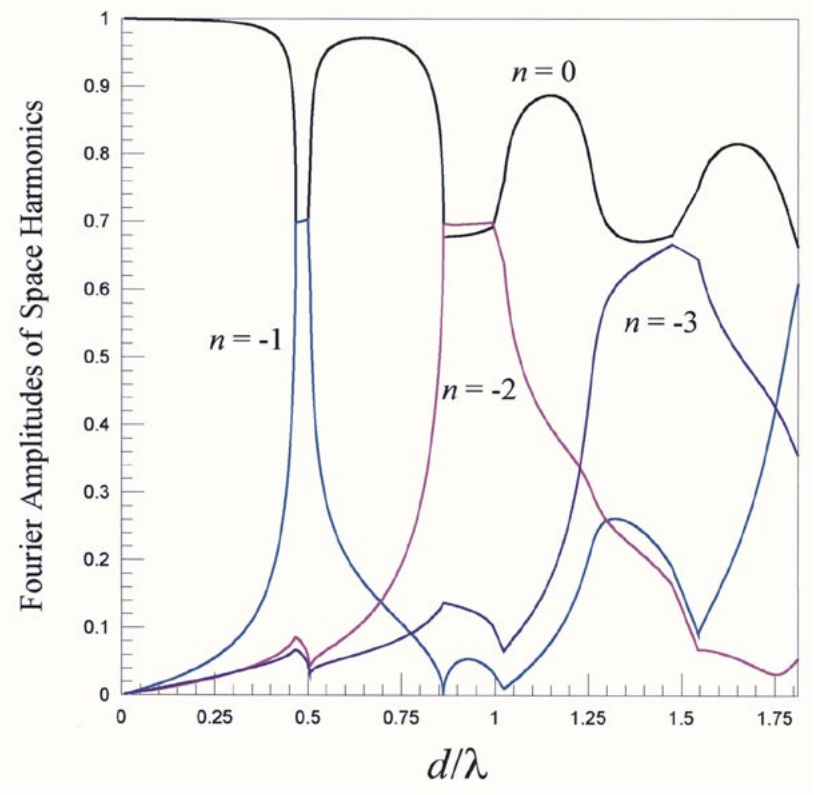

Fig. 5. Variation of amplitudes of space harmonics against normalized frequency $k_o d/2\pi$ for the corrugated metal surface with the parameters: $h = 0.21d$and $a = d$.

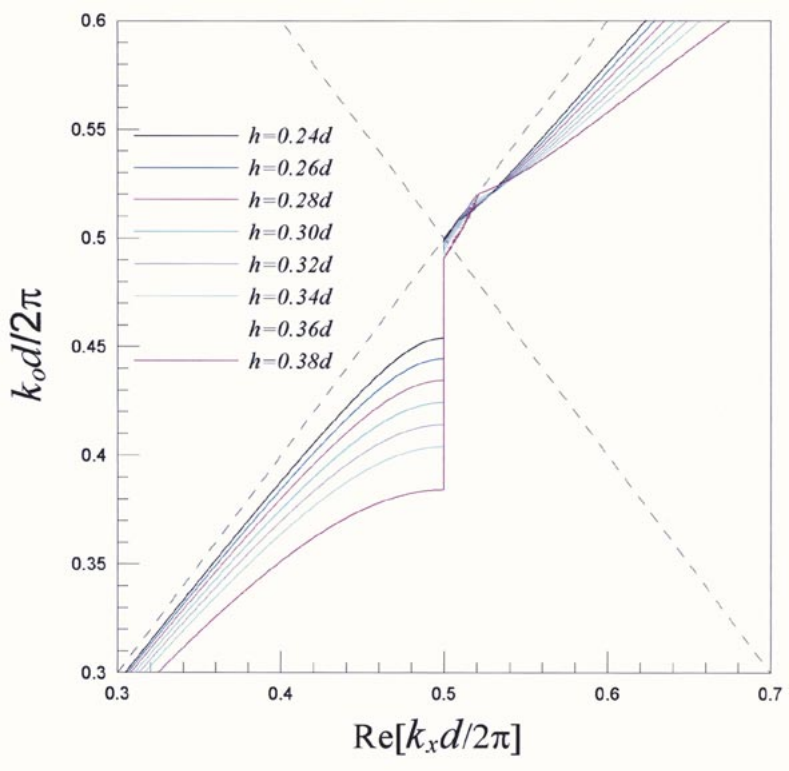

Fig. 6. Variation of the width of stopband with respect to the structure heights for the case of $a = d$.

resulting in a single stopband, instead of two separate ones. A similar explanation may be given to the stopbands around the points B and C in Fig. 3 and they can be related back to the pair B and B′ and the pair C and C′, respectively.

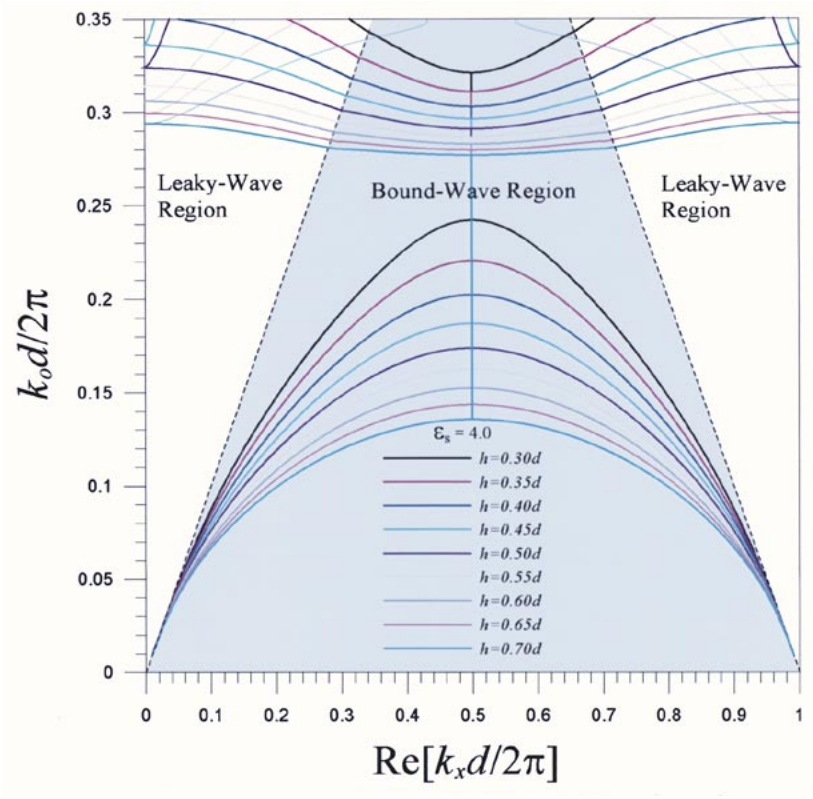

(a)

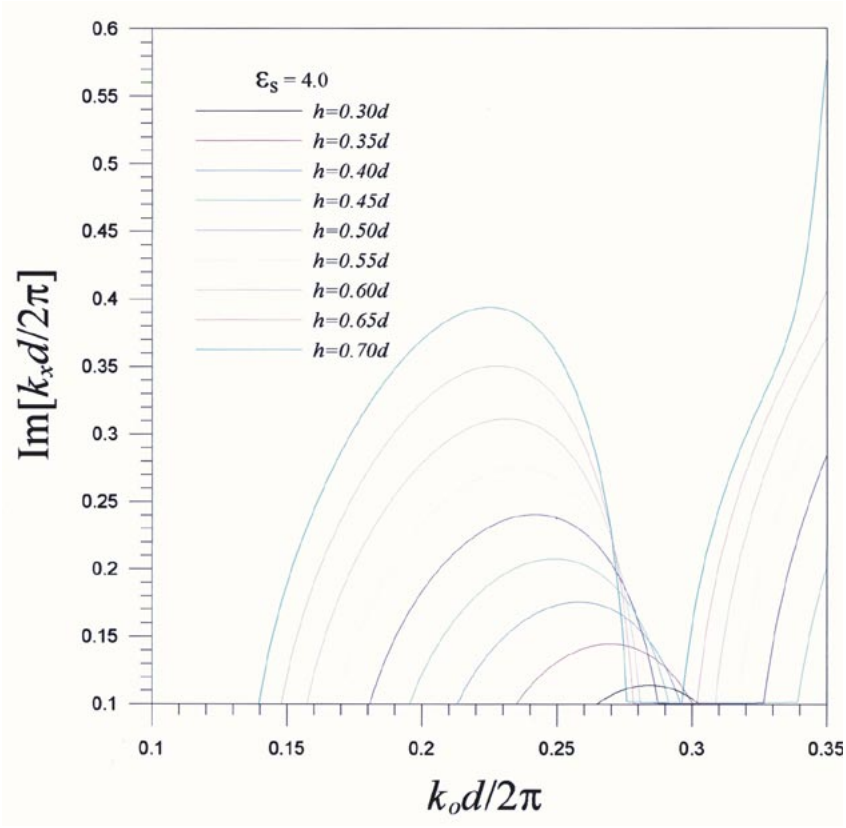

(b)

Fig. 7. The behavior of stopbands for various thickness of corrugates; (a) normalized propagation constant $\mathrm{Re}[k_x d/2\pi]$ and (b) normalized attenuation constant $\mathrm{Im}[k_x d/2\pi]$.

To substantiate the explanations described above, we plot the amplitudes of the first four modes of the parallel-plate waveguides in Fig. 4. In the low frequency range, the fundamental mode is obviously dominant, but the contribution from

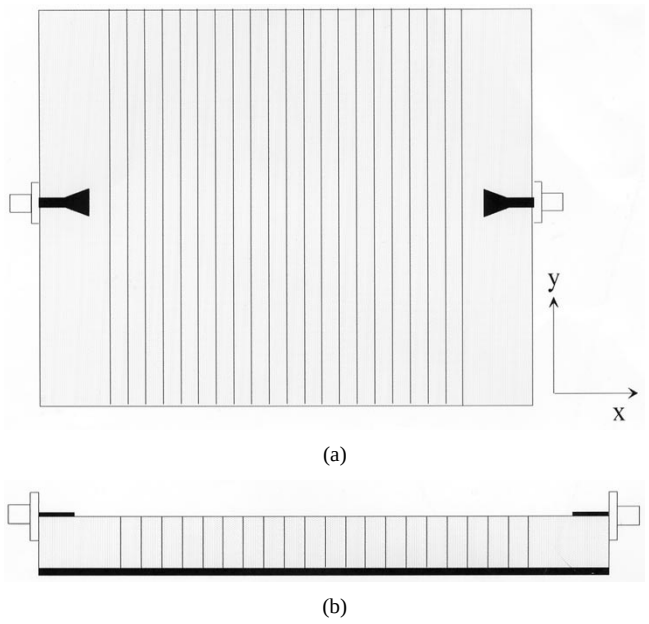

Fig. 8. Structural configuration of experiment setup.

the next higher-order mode, $m = 1$, increases significantly with increasing frequency. Toward the normalized frequency $k_o d/2\pi = 0.5$, we see a sudden switch of domination from the fundamental mode to the next higher mode. A similar behavior occurs also around the frequencies $k_o d/2\pi = 1.0$ and 1.5. This demonstrates the effect of the structural resonance, and suggests the utilization of the mode switching for the design of the dispersion characteristics of a periodic structure.

For both surface-wave and leaky-wave applications, the amplitudes of the space harmonics are very important, because they determine the efficiency of excitation for surface waves. Fig. 5 shows the variation of the harmonic amplitudes V_{-3}, V_{-2}, V_{-1} and V_0 vs. the normalized frequency. We recall that $V{-}n$ is the amplitude of $-n$th space harmonic at the air-corrugate interface, $z = h$. It is noted that these curves have rapid variations close to the stopband edges. Due to the contra-flow interaction, the interchange of energy between two space harmonics will be taken place around the stopbands, as marked by A, B and C. Also noted is that the $|V_{-1}| = |V_0|$ within the stopband A in the bound-wave region. However, beyond the bound-wave triangular, one or more higher space harmonics $(n \neq 0)$ may be propagating in the air region and carry away energy from the structure, the two interacting space harmonics may no longer have equal amplitudes within the stopbands B and C.

In Fig. 3, the first stopband is in the bound-wave region and it will be good for the application to the suppression of surface waves. In an attempt to increase the width of the stopband in the bound-wave region, we try to evaluate the effect of the structure height on the width of the first stopband and the results are shown in Fig. 6. Here, we can achieve a bandwidth of over 20% of the operating frequency, while still keeping the operation with a single mode.

Based on the definition of the relative bandwidth for stop band referring to [13], we designate the relative bandwidth BW as the ratio of upper band edge to lower band edge, that is, $BW = NF_U/NF_L$, where NF is defined as the normalized frequency, d/λ, of a stop band. NF_U and NF_L are the upper and lower band edges of the stop band. Since the upper edge of the stop band is around 0.5 for each case, the relative bandwidth can be written as $BW = 0.5/NF_L$. After using the technique of the curve fitting in a least-squares sense for the locations of band edges for each case, as shown in the Fig. 6, the relation between the NF_L and the height of corrugation, h, can be explicitly written as:

$$h = (1.1563 - 2.0187NF_L)d \tag{7}$$

In doing so, we can achieve a rule of thumb to design a structure of desired. For example, if we would like to have a structure having the relative bandwidth X, the lower band edge of normalized frequency is $NF_L = 0.5/X$. Since the start frequency (wavelength) of stop band is usually given by a certain design specification, the period d can be obtained by $d = 0.5\lambda/X$, where λ is the start wavelength. Substitution of NF_L and the period d into (7), we can determine the height of the corrugation to build up the corrugated metal surface of desired.

In addition to the corrugated metal surface in the previous example, we have also investigated the same metal structure that is filled with a dielectric medium, with the relative dielectric constant $\varepsilon_s = 4.0$ in the parallel-plate region. Fig. (7a) shows the variation of the stopbands for various thicknesses of the corrugation. We observe that the behavior of the dispersion curves is getting flatter and the stopband is getting wider as the thickness h is increased. To put it differently, the increase of h will lead to the increase of input impedance, so that the stopband will begin at a low frequency. This permits us to achieve a design of compact periodic structure by using the phenomena of strong structure dispersion. Fig. (7b) shows the variation of the normalized attenuation constant $\mathrm{Im}[k_x d/2\pi]$ vs. the normalized frequency with the corrugation thickness, h, as a parameter. The stopband behavior is very important for the operation of surface wave suppression and the maximum value of attenuation constant determines the minimum length required for eliminating most of the surface waves. Since the maximum of the attenuation constant is so large for the case of strong structure dispersion, we do not need many periods of the structure to achieve the desired degree of surface wave suppression. This again proves the possibility of a compact size of a resonance-type periodic structure.

V. Measurement for the Transmission of Surface Wave

In order to verify the dispersion characteristics obtained by the numerical computation, we have setup an experiment to measure the transmission characteristics of the surface wave on the resonance type periodic structure. Fig. 8 shows the experimental setup with the top and side views of a corrugated structure that is periodic in the x direction and is uniform in the y direction. Each cavity may be viewed as a parallel-plate waveguide that is completely short-circuited at one end, open at the other end and filled with a uniform dielectric medium. The thickness and relative dielectric constant of the substrate is 1.54 mm and 4.0, respectively. The period of the metal fins along the x direction is 3.5 mm. The length of each metal fin along *y* direction is 100 mm. We have utilized the horn-type antennas that

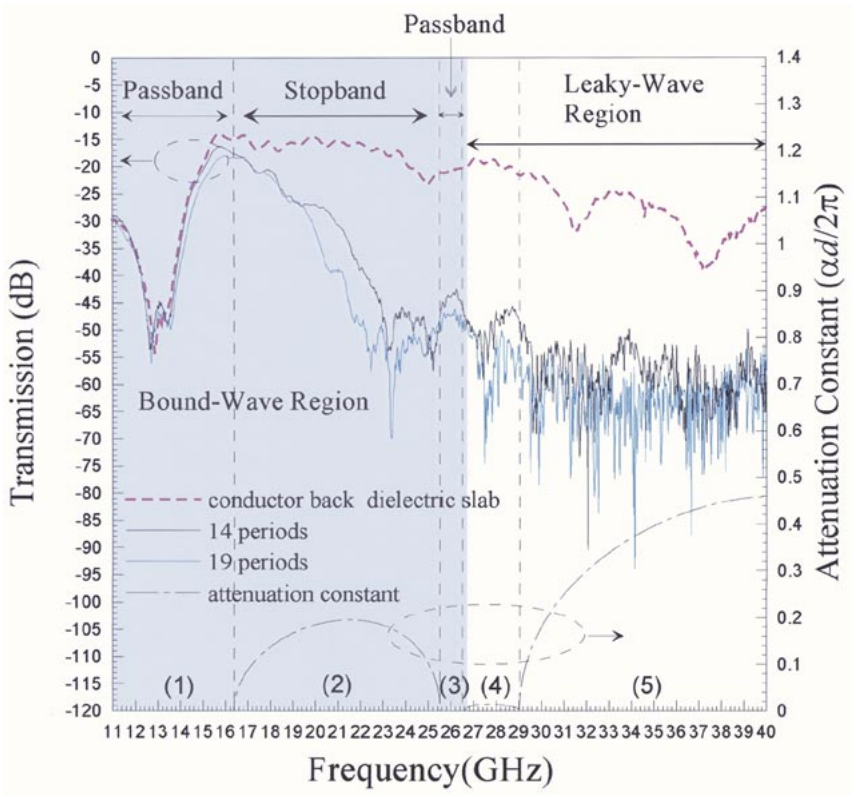

Fig. 9. Measurement data for the transmission of surface wave on a resonance-type periodic structure; for the case of $d = 3.5$ mm, $h = 1.54$ mm, $\varepsilon = 4.0$.

are printed on two opposite ends of the periodic structure to excite and receive the surface wave. Here, the tapered microstrips will provide a smooth transition for the quasi-TEM mode from the narrow end to the wide end, so that we can excite effectively a TM surface wave with flat wave front.

Due to the finite size of the structure, the surface wave may be reflected and diffracted by the edges of the structure; it may cause the multipath interference and result in the variation of the measured transmission data. To distinguish the dispersion characteristics from the effect of multipath, we had fabricated a uniform structure that has the same geometric and material parameters but without corrugates to act as a reference in order to characterize accurately the wave phenomena in periodic structure. Moreover, to reduce the effect multipath interference, we had taper the edges of the substrate to make a smooth transition of surface wave to radiate away from the structure.

Fig. 9 shows the measured TM surface-wave transmission data. Here, the curve in the dashed line is for the surface-wave transmission through the uniform structure. The curves in black and blue are those for the structure with 14 and 19 periods, respectively. Also shown in Fig. 7 is the normalized attenuation constant $\alpha d/2\pi$ against the normalized frequency from theoretical computation. Inside the bound-wave region where it is highlighted, we have a stopband marked by Region (2) that is sandwiched between two passbands marked by Region (1) and (3), respectively. In the higher frequency range, we have the leaky-wave region that is divided into two subregions, as marked by Region (4) and (5), respectively. In the low frequency range, the effect of periodicity is insignificant and the periodic structure behave like a uniform one; therefore, the three curves are close to one another. As the operation frequency is increased to enter into Region (2), stopband region, the transmission drops drastically. This is due to the effect of Bragg reflection in bound-wave region. Because the large value of the attenuation constant is in the range close to the upper edge of the stopband, the drops in transmission are strong there. Beyond Region 2, the attenuation constant returns to zero and then enters into the passband region, where the transmission should increase; though not very pronounced, it is verifiable by the results in Region 3. Beyond Region 3, the dispersion curve enters into the leaky-wave region where the surface wave start to leak into the air region, and then the transmission start to drop. Near the edge of Region 4, the attenuation constant returns to zero again. This can be verified by the increase of the transmission in Region 4. As the operation frequency continues to increase to enter into Region 5, the attenuation constant become so large that the transmission data drop consistently over the entire range of frequency investigated. Furthermore, the increase of the number of periods does reduce the transmission, and this can be easily seen from our measured transmission data as shown.

VI. Conclusion

We have presented a systematical treatment of guided waves on a corrugated metal surface. Numerical results are carried out and are displayed in the form of the Brillouin diagram. In order to identify the wave interactions and to show the stopband structure of the dispersion curves, the amplitude distribution of the waveguide modes are also presented. The approxi-

mation of a resonance-type periodic structure by an impedance surface is examined and a simple criterion is suggested, so that the frequency dispersion of the impedance surface may be accounted for by switching from one waveguide mode to another in a single-mode approximation. The effect of the structural dispersion on the Bragg phenomenon is carefully evaluated, and it is demonstrated that a wide stopband can be achieved with a proper design of the resonance-type periodic structure.

ACKNOWLEDGMENT

The authors thank Mr. C. H. Cheng, H. Y. Shih, and I. C. Wu for their help in doing the experiments. They also express their appreciation to the reviewers for their useful comments in revising this paper.

REFERENCES

[1] W. Rotman, "A study of single surface corrugated guides," *Proc. I.R.E.*, vol. 39, pp. 952–959, Aug. 1951.
[2] R. S. Elliott, "On the theory of corrugated plane surfaces," *IRE Trans. Antennas Propagat.*, pp. 71–81, Apr. 1954.
[3] R. A. Hurd, "The propagation of an electromagnetic wave along an infinite corrugated surface," *Can. J. Phys.*, vol. 32, pp. 727–734, 1954.
[4] L. A. Vainshtein, "Propagation of electromagnetic waves on a corrugated surface," *Soviet Phys.-Tech. Phys. 1*, p. 379, 1956.
[5] J. Ehrlich and L. L Newkirk, "Corrugated surface antennas," in *Proc. IRE Nat. Conv. Rec.*, Mar. 1953, pp. 18–33.
[6] R. W. Houghardy and R. C. Hansen, "Scanning surface wave antennas—oblique surface waves over corrugated conductor," *IRE Trans. Antennas Propagat.*, vol. 6, pp. 370–376, Oct. 1958.
[7] R. E. Collin, "Properties of slotted dielectric interfaces," *IRE Trans. Antennas Propagat.*, pp. 274–276, Jan. 1959.
[8] L. O. Goldstone and A. A. Oliner, "A note on surface waves along corrugated structures," *IRE Trans. Antennas Propagat.*, vol. 7, pp. 62–73, July 1959.
[9] T. Morita and S. B. Cohn, "Microwave lens matching by simulated quarter-wave transformers," *IRE Trans. Antennas Propagat.*, vol. 4, pp. 33–39, Jan. 1956.
[10] V. H. Rumsey, *Electromagnetic Theory and Antennas*, E. C. Jordan, Ed. New York: Macmillan, 1963.
[11] P.-S. Kildal, "Artificially soft and hard surfaces in electromagnetics," *IEEE Trans. Antennas Propagat.*, vol. 38, pp. 1537–1544, Oct. 1990.
[12] P.-S. Kildal, A. A. Kishk, and A. Tengs, "Reduction of forward scattering from cylindrical objects using hard surfaces," *IEEE Trans. Antennas Propagat.*, vol. 44, pp. 1509–1520, Nov. 1996.
[13] Z. Ying, P.-S. Kildal, and A. A. Kishk, "Study of different realizations and calculation models for soft surfacees by using a vertical monopole on a soft disk as a test bed," *IEEE Trans. Antennas Propagat.*, vol. 44, pp. 1474–1481, Nov. 1996.
[14] G. P. Gauthier, A. Courtay, and G. M. Rebeiz, "Microstrip antennas on synthesized low dielectric-constant substrates," *IEEE Trans. Antennas Propagat.*, vol. 45, pp. 1310–1314, Aug. 1997.
[15] G. M. Papapolymerou, R. F. Drayton, and L. P. B. Katechi, "Micromachined patch antennas," *IEEE Trans. Antennas Propagat.*, vol. 46, pp. 275–283, Feb. 1998.
[16] V. M. Lubecke, K. Mizuno, and G. M. Rebeiz, "Micromachining for terahertz applications," *IEEE Trans. Microwave Theory Tech.*, vol. 46, pp. 1821–1831, Nov. 1998.
[17] D. Sievenpiper, L. Zhang, R. F. Jimenez Broas, N. G. Alexopolous, and E. Yablonovitch, "High-impedance electromagnetic surface with a forbidden frequency band," *IEEE Trans. Microwave Theory Tech.*, vol. 47, pp. 2059–2074, Nov. 1999.
[18] F.-R. Yang, K.-P. Ma, Y. Qian, and T. Itoh, "A novel TEM waveguide using uniplanar compact photonic-bandgap (UC-PBG) structure," *IEEE Trans. Microwave Theory Tech.*, vol. 47, pp. 2092–2098, Nov. 1999.
[19] F. R. Yang, K.-P. Ma, Y. Qian, and T.Tatsuo Itoh, "A Uniplanar Compact Photonic Band-gap (PBG) structure and its application for microwave circuits," *IEEE Trans. Microwave Theory Tech.*, vol. 47, pp. 1509–1514, Aug. 1999.
[20] R. B. Hwang and S. T. Peng, "Guidance characteristics of two-dimensional periodic impedance surface," *IEEE Trans. Microwave Theory Tech.*, vol. 47, pp. 2503–2511, Dec. 1999.
[21] R. B. Hwang and S. T. Peng, "Guided waves on 2-D periodic structures and their relation to planar photonic band gap structures," *IEICE Trans. Electron.*, vol. E83-C, no. 5, pp. 705–712, May 2000.

Ruey Bing Hwang (M'96) was born in Nan-Tou, Taiwan, R.O.C., on January 20, 1967. He received the B.S.degree in communication engineering from National Chiao-Tung University, Hsinchu, Taiwan, R.O.C., in 1990, the M.S. degree from the Institute of Electrical Engineering, National Taiwan University, Taipei, Taiwan, R.O.C., in 1992, and the Ph.D. degree the Institute of Electronics, National Chiao-Tung University, in 1990, 1992, and 1996, respectively.

From 1996 to 1999, he was with the National Center for High-Performance Computing, Hsinchu, where he worked on computational electromagnetics. From 1999 to the spring of 2003, he was an Associate Researcher Professor at the Microelectronics and Information Systems Research Center, National Chiao-Tung University. In the spring of 2003, he joined the Graduate Institute of Communication Engineering, National Chi Nan University, Nan-Tou, Taiwan, R.O.C., as an Associate Professor. His professional interests include the scattering and guiding characteristics of artificial crystal waveguides, photonic band-gap structures and grating couplers, array antenna design and electromagnetic compatibility.

Dr. Hwang is a Member of Phi Tau Phi.

Song Tsuen Peng (M'74–SM'82–F'88), biographical information not available at the time of publication.